Mcm4 C-terminal domain of MCM helicase prevents excessive formation of single-stranded DNA at stalled replication forks

Naoki Nitani, Chie Yadani, Hayato Yabuuchi, Hisao Masukata, and Takuro Nakagawa*

Department of Biological Sciences, Graduate School of Science, Osaka University, 1-1 Machikaneyama, Toyonaka, Osaka 560-0043, Japan

Edited by Richard D. Kolodner, University of California at San Diego School of Medicine, La Jolla, CA, and approved June 25, 2008 (received for review May 31, 2008)

The minichromosome maintenance (MCM) helicase, composed of subunits Mcm2–7, is essential for the initiation and elongation phases of DNA replication. Even when DNA synthesis is blocked, MCM continues DNA unwinding to some extent for activation of the replication checkpoint and then stops. However, the mechanism of regulation of MCM-helicase activity remains unknown. Here, we show that truncation of the Mcm4 C-terminal domain (CTD) in fission yeast results in hypersensitivity to replication block caused by dNTP depletion. The truncation *mcm4-c84* does not affect the activation of the replication checkpoint pathway but delays its attenuation during recovery from replication block. Two dimensional gel electrophoresis showed that *mcm4-c84* delays the disappearance of replication intermediates, indicating that the Mcm4 CTD is required for efficient recovery of stalled replication forks. Remarkably, chromatin immunoprecipitation revealed that *mcm4-c84* brings about an increase rather than a decrease in the association of the single-stranded DNA-binding protein RPA to stalled forks, and MCM and the accessory complex GINS are unaffected. These results suggest that the Mcm4 CTD is required to suspend MCM-helicase activity after the formation of single-stranded DNA sufficient for checkpoint activation.

replication checkpoint | protein kinase | DNA unwinding | hydroxyurea | RPA

In each cell cycle, complete and accurate duplication of chromosomal DNA is important for the faithful transmission of genetic information to the daughter cells and for the suppression of genome instability (1). The minichromosome maintenance (MCM) complex is a DNA helicase that is essential for the initiation and elongation phases of DNA replication (2, 3). During early G1, MCM is loaded onto replication origins in a Cdt1- and Cdc18/Cdc6-dependent manner to form the prereplicative complex (pre-RC). Before the initiation of replication, other replication factors, including the Cdc45 and GINS complexes, are recruited to the pre-RC. During the elongation of replication, MCM, with the aid of Cdc45 and GINS, unwinds double-stranded DNA to produce single-stranded templates for DNA synthesis (4–6). In mice, deregulated expression of MCM7 accelerates tumor formation (7, 8). A hypomorphic mutation of MCM4 causes chromosome instability and mammary adenocarcinomas (9). These observations demonstrate that the MCM helicase is involved in suppressing genome instability and cancer.

The elongation of replication can be blocked by DNA damage, tight binding of the protein to DNA, or dNTP depletion (10, 11). The replication block caused by hydroxyurea (HU), an inhibitor of ribonucleotide reductase that is required for dNTP synthesis, leads to the activation of the replication-checkpoint pathway. The replication checkpoint induces cell-cycle arrest and prevents the collapse of stalled forks (12, 13). In the fission yeast *Schizosaccharomyces pombe*, the kinase Rad3/ATR is the central player in the DNA structure checkpoint, and Cds1/Chk2 and Chk1 are integral kinases in the replication- and DNA damage-checkpoint pathways, respectively (14, 15). MCM is implicated in the activation of the replication checkpoint in two ways: the formation of replication forks and the extension of single-stranded DNA (ssDNA). A sufficient number of stalled replication forks are required for full activation of the checkpoint kinase (16–18). DNA unwinding at the fork continues to some extent even after replication is blocked to extend ssDNA (19). ssDNA coated by multiple RPAs is a key structure required for checkpoint activation (20, 21); however, eventually DNA unwinding stops. Otherwise, excessive ssDNA would be produced, thereby impeding the resumption of fork progression during recovery from the replication block. However, little is known about the mechanism of regulation of the unwinding activity of MCM helicase.

Eukaryotic MCM consists of six different polypeptides (Mcm2–7); however, a single species of Mcm polypeptide forms a complex in archaea, suggesting that the archaeal Mcm holds all fundamental activities of MCM. Phylogenetic comparison revealed that Mcm4 represents the most ancient form of eukaryotic Mcm (22). Here, we show that the C-terminal domain (CTD) of Mcm4, which is conserved from archaea to humans, prevents excessive formation of ssDNA when replication is blocked by dNTP depletion.

Results

The Mcm4 CTD Plays an Important Role When Elongation of Replication Is Blocked by dNTP Depletion. Archaeal Mcm is divided into three domains, all of which are conserved in the Mcm4 of *S. pombe* and *Homo sapiens* (Fig. 1*A*). A central AAA$^+$ domain (23) is important for helicase activity. The N-terminal domain (NTD) of archaeal Mcm forms ring-like complexes and exhibits DNA binding activity (24), whereas the role of its CTD remains to be clarified. To reveal the role of the Mcm4 CTD, fission-yeast strains expressing C-terminally truncated versions of Mcm4 were created. A serial dilution assay revealed that deletion of 106 amino acids (*mcm4–c106*) exhibited a temperature-sensitive phenotype, whereas deletion of 70 or 84 residues (*mcm4–c70* or *mcm4–c84*) caused no apparent growth defects at any of the temperatures examined (Fig. 1*B Upper*). In addition, the doubling times determined at 30°C for *mcm4–c70* and *mcm4–c84* cells (2.56 ± 0.04 and 2.53 ± 0.03 h, respectively) were indistinguishable from that of wild-type cells (2.56 ± 0.06 h). However, the *mcm4* mutant cells exhibited hypersensitivity to HU when compared with wild-type cells (Fig. 1*B Lower*). Because

Author contributions: N.N. and T.N. designed research; N.N., C.Y., and T.N. performed research; H.Y. contributed new reagents/analytic tools; N.N., C.Y., and T.N. analyzed data; and N.N., C.Y., H.M., and T.N. wrote the paper.

The authors declare no conflict of interest.

This article is a PNAS Direct Submission.

*To whom correspondence should be addressed. E-mail: takuro4@bio.sci.osaka-u.ac.jp.

This article contains supporting information online at www.pnas.org/cgi/content/full/0805307105/DCSupplemental.

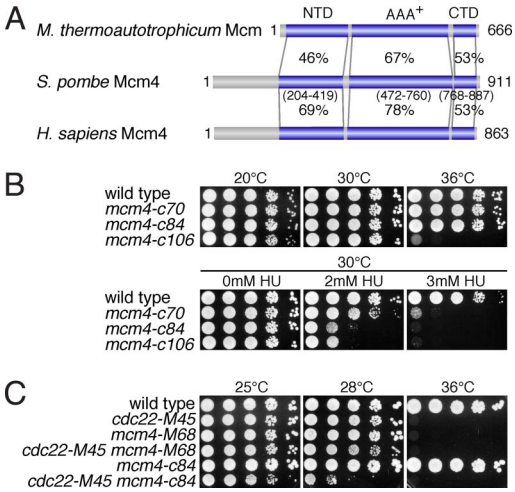

Fig. 1. The Mcm4 CTD plays an important role when replication is blocked by dNTP depletion. (*A*) Comparison between archaeal Mcm (*Methanobacterium thermoautotrophicum*) and eukaryotic Mcm4 (*S. pombe* and *H. sapiens*). Amino-acid similarities between the Mcm proteins are indicated for the AAA$^+$, NTD, and CTD. (*B*) Temperature and HU sensitivity of wild-type (TNF34), *mcm4–c70* (TNF1312), *mcm4–c84* (TNF598), and *mcm4–c106* (TNF599) strains. The log-phase cells were serially diluted 10-fold with distilled water and plated onto YE plates supplemented with the indicated concentrations of HU. (*C*) The *mcm4–c84* mutation lowers the restriction temperature of *cdc22–M45* cells. Wild-type, *mcm4–c84*, *mcm4–M68* (TNF907), *cdc22–M45* (TNF2251), *mcm4–c84 cdc22–M45* (TNF2254), and *mcm4–M68 cdc22–M45* (TNF2187) log-phase cells grown at 25°C were serially diluted 10-fold and spotted onto YE plates as described above. The plates were incubated at the temperatures indicated above the images.

mcm4–c84 and *mcm4–c106* cells exhibited similar degrees of sensitivity to HU, we used *mcm4–c84* for further analysis. To determine whether the observed HU sensitivity was because of dNTP depletion, the dNTP pool was reduced by an alternative method that used the temperature-sensitive *cdc22–M45* mutant. Cdc22 is a large subunit of ribonucleotide reductase (25). Introduction of the *mcm4–c84* mutation into *cdc22–M45* cells strongly enhanced the temperature-sensitive growth defect (Fig. 1*C Center*). The *mcm4–M68* (*cdc21–M68*) mutation causes an amino-acid substitution (Leu238Pro) and confers a temperature-sensitive growth defect (26). In contrast to *mcm4–c84*, *mcm4–M68* only slightly impaired the growth of *cdc22–M45* cells. Allele specificity was also observed for HU sensitivity (data not shown). These data demonstrate that the CTD of Mcm4 plays an important role when replication is blocked by dNTP depletion.

The Mcm4 CTD Is Not Essential for Activation of the Replication Checkpoint Pathway. When cells are treated with HU, replication forks are stalled and the replication-checkpoint cascade is induced. In fission yeast, Rad3 kinase is activated and phosphorylates Cds1 kinase, which in turn phosphorylates various target proteins, including the structure-specific nuclease Mus81 (27–29). To determine whether the Mcm4 CTD is required for checkpoint activation, HU-induced phosphorylation of Cds1 and Mus81 was examined by using a gel mobility shift assay (14, 15, 28). Extracts prepared from wild-type, *mcm4–c84*, and *cds1*Δ cells expressing Mus81-myc were separated by SDS-PAGE and transferred onto a membrane. Immunostaining for Cds1 revealed that the protein mobility was equally retarded in wild-type and *mcm4–c84* cells in response to HU treatment (Fig. 2*A*). Mus81-myc, detected by using anti-myc antibodies, was also retarded in wild-type and *mcm4–c84*, but not in *cds1*Δ cells (Fig. 2*A*). To measure Cds1 activity, we carried out an *in vitro* kinase assay (15) in which GST-Wee1 purified from bacteria was

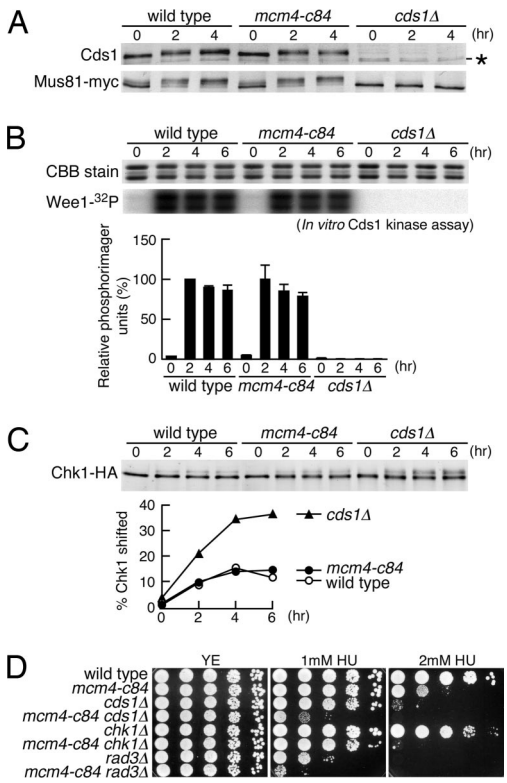

Fig. 2. The Mcm4 CTD is not required for activation of the replication checkpoint. (*A*) Gel mobility shift assay for Cds1 and Mus81 proteins. Log-phase cells of wild-type (TNF1477), *mcm4–c84* (TNF2286), and *cds1*Δ (TNF1935) in Edinburgh minimal medium (EMM) were treated with 12 mM HU for 0, 2, or 4 h. A total of 1.5 μg of the extracts was loaded onto 10% SDS/PAGE (acrylamide:bis-acrylamide = 200:1) to detect Cds1 (upper gels) and Mus81-myc (lower gels). Rabbit serum against Cds1 (provided by T. S. Wang, Stanford University, Stanford, CA) and the anti-myc antibody (9E11; Medical and Biological Laboratories) were used at a dilution of 1:2,000. The band marked with an asterisk indicates a nonspecific species. (*B*) *In vitro* kinase assay for Cds1. Exponentially growing wild-type (TNF422), *mcm4–c84* (TNF1575), and *cds1*Δ (TNF609) cells were treated with 12 mM HU for 0, 2, 4, or 6 h. A total of 1.5 mg of the yeast extract and GST-Wee1^{70} prepared from *Escherichia coli* were mixed and subjected to kinase reactions that contained [γ-^{32}P]ATP to probe the phosphorylated proteins. The reaction products were separated by 12% SDS-PAGE (29:1), the GST-Wee1^{70} was visualized by CBB staining (CBB stain, *Upper*), and the phosphorylated proteins were detected by using a phosphorimager (Wee1-^{32}P, *Upper*). The relative intensities of the phosphorimager signal of Wee1-^{32}P are indicated (*Lower*). The values represent the mean of two independent experiments; the error bars represent the standard deviation. The two protein bands detected in each lane may be the degradation products of GST-Wee1. (*C*) Mobility shift assay for Chk1 protein. Log-phase cells of wild-type (TNF422), *mcm4–c84* (TNF1575), and *cds1*Δ (TNF609) in EMM were treated with 12 mM HU for 0, 2, 4, or 6 h. A total of 2.0 μg of the yeast extracts was loaded onto 8% SDS-PAGE (59:1) and transferred onto a nylon membrane. Hemagglutinin (HA)-tagged Chk1 was detected by immunostaining with the anti-HA antibody (16B12; Covance Research Products). The proportion of a shifted species of Chk1 to the total amount of Chk1 is plotted. (*D*) Log-phase cells of wild-type (TNF34), *mcm4–c84* (TNF598), *cds1*Δ (TNF256), *mcm4–c84 cds1*Δ (TNF1395), *chk1*Δ (TNF1158), *mcm4–c84 chk1*Δ (TNF1548), *rad3*Δ (NNF61), and *mcm4–c84 rad3*Δ (TNF1464) strains in EMM were serially diluted 10-fold and plated onto YE plates supplemented with the indicated concentrations of HU. The yeast cells were grown at 30°C.

phosphorylated in a Cds1-dependent manner in the presence of [γ-^{32}P]ATP. After separation of the reaction product by SDS-PAGE, the proteins were stained with Coomassie brilliant blue (CBB) and the radioactive signals were detected by using a phosphorimager (Fig. 2*B*). GST-Wee1 phosphorylation was increased to the same level in wild-type and *mcm4–c84* cells after

the addition of HU. In *cds1*Δ cells, Wee1 phosphorylation was only observed at the background level. These *in vivo* and *in vitro* data show that the *mcm4–c84* mutant is proficient in activation of the replication checkpoint. Cds1 and Chk1 are activated primarily in response to replication block and DNA damage, respectively; however, in the absence of Cds1, Chk1 becomes activated by HU treatment, probably because of the conversion of stalled forks to damaged DNA (e.g., double-strand breaks) (14, 15). We reasoned that if the Mcm4 CTD was involved in the replication-checkpoint response downstream of Cds1 activation, hyperactivation of Chk1 would occur; however, immunostaining for Chk1-HA revealed that an HU-induced mobility shift was suppressed similarly in wild-type and *mcm4–c84* cells compared with *cds1*Δ cells (Fig. 2*C*). Consistent with these findings, *mcm4–c84 cds1*Δ cells exhibited increased sensitivity to HU compared with either of the single mutants (Fig. 2*D*). Increased sensitivity was also observed in case of *mcm4–c84 chk1*Δ and *mcm4–c84 rad3*Δ cells. Collectively, these data show that Mcm4 CTD is not required for activation of the replication checkpoint.

Attenuation of the Replication Checkpoint Is Delayed by Truncation of the Mcm4 CTD. Recovery from the replication block was examined by monitoring cell-cycle progression. Treatment of the *mcm4–c84* and wild-type cells with HU suppressed the formation of the septum and caused the cells to become elongated [supporting information (SI) Fig. S1]. After incubation for 3 h in the presence of HU, the cells were washed with sterilized water and resuspended in HU-free media, allowing resumption of the cell cycle (Fig. 3*A*). In wild type, septa started to appear at 60 min and peaked at 100 min after the removal of HU. The *mcm4–c84* mutation delayed septum formation by ≈20 min. The observed delay suggests that the replication checkpoint remains active even after the removal of HU. To test this possibility, we performed a Cds1 kinase assay using the extract prepared after HU removal. To improve the sensitivity of the assay, *cdc25-22* background strains were temporally incubated at 36°C to induce G2 arrest, followed by incubation at 25°C for 2 h in the presence of HU to synchronously block replication (Fig. 3*B*). The cells were then washed and resuspended in HU-free media to allow recovery from the replication block. Measurement of the kinase activity revealed that *mcm4–c84* causes a delay in the attenuation of Cds1 activity after release from the replication block (Fig. 3*C*).

The Mcm4 CTD Is Required for Efficient Resumption of Fork Progression During Recovery from the Replication Block. Considering that stalled replication forks are the structures that are essential for activation of the replication checkpoint (16, 17), the forks might have persisted after the removal of HU in *mcm4–c84* cells. To test this possibility, replication intermediates were detected by a neutral-neutral 2D gel electrophoresis assay (30) using synchronous cultures of the *cdc25-22* background strains. Chromosomal DNA was prepared in agarose plugs, digested with *Eco*T22I, separated by 2D gel electrophoresis, and transferred onto a nylon membrane. A 6.4-kb fragment encompassing a replication origin, *ori2004*, on chromosome II (Fig. 4*A*) was detected by Southern blotting. The bubble arcs represent the origins that have fired bidirectionally within the restriction fragment, whereas the Y arcs result from the asymmetric progression of replication forks that have passed one end of the fragment (Fig. 4*B*). Cone signals are thought to consist of reversed and converging forks, whereas spike signals represent cruciform DNA (12, 20, 31). Because the two signals overlapped, we measured their sum as the cone+spike signal in this study. When cells were allowed to enter S phase synchronously in the absence of HU, similar amounts of replication intermediates were detected transiently in early S phase in wild-type and *mcm4–c84* cells (Fig. 4*C*). Thus, it appears that the *mcm4–c84* mutation minimally, if at all, affects the initiation and elongation of replication under

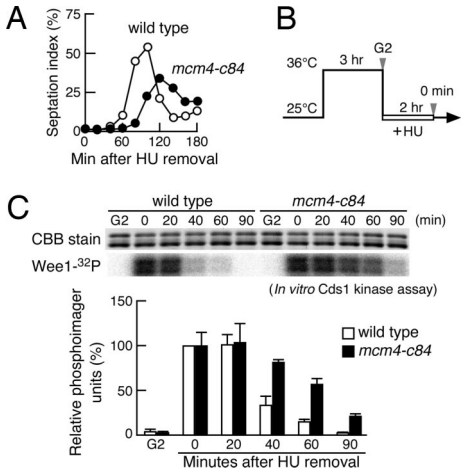

Fig. 3. The *mcm4–c84* mutation delays the resumption of the cell cycle and attenuation of Cds1 kinase after release from replication block. (*A*) Exponentially growing wild-type (TNF34) and *mcm4–c84* (TNF598) cells in EMM were treated with 12 mM HU for 3 h at 30°C. After incubation in the presence of HU, the cells were washed with distilled water and transferred to HU-free EMM medium. A total of 1.0 ml of culture was harvested at the indicated time points and stored at 4°C in 70% ethanol. The percentage of cells containing septa, indicative of passage through mitosis, is shown. At each time point, at least 500 cells were examined by microscopy, and the cells containing the septum that was stained with calcofluor, were counted. (*B*) Schematic diagram of the incubation conditions for *cdc25-22* cultures to assess the recovery from an HU-induced replication block. The yeast culture was grown at 25°C until log phase; the incubation temperature was then raised to 36°C for synchronization in G2 phase. After incubation for 3 h at 36°C, 10 mM HU was added, and the temperature was decreased to 25°C, allowing synchronous progression into S phase. After incubation for 2 h, HU was removed from the culture by filtration, and the cells were washed and resuspended in HU-free EMM and incubated at 25°C. The cells were harvested at the temperature shift-down (G2) and at the indicated time points after removal of HU. (*C*) Cds1 kinase activity of wild-type (TNF701) and *mcm4–c84* (TNF1687) strains after removal of HU was measured as described in Fig. 2. The relative intensity of the phosphorimager signals of Wee1 is indicated. The plotted values represent the mean of three independent experiments; the error bars show the standard deviation.

an unperturbed condition. When replication was blocked by HU treatment, the replication intermediates accumulated in wild-type and *mcm4-c84* cells to a similar level (Fig. 4*D*, 0 min). After the removal of HU, the intermediates disappeared within 60 min in wild-type cells; however, the Y arc and the cone+spike signals were still detected in *mcm4–c84* cells even after 60 min of incubation. We further examined the replication intermediates in the region that contains no origins (Fig. 4*E*). As expected, bubble arcs were not observed in this fragment (Fig. 4*F*). In the presence of HU, the accumulated replication intermediates were less abundant in *mcm4–c84* compared with wild-type cells (Fig. 4*F*, 0 min). Considering that replication forks progress slowly even in the presence of HU (20), a fraction of the replication forks may not have reached this origin-free region in *mcm4–c84* cells because of a defect in the resumption of fork progression. After HU removal, the replication intermediates disappeared within 60 min in wild-type cells, whereas they were still detected in *mcm4–c84* cells even after incubation for 90 min. These data suggest that the Mcm4 CTD is required for efficient resumption of fork progression during recovery from the replication block.

The Mcm4 CTD Prevents Excessive Formation of ssDNA at the Stalled Replication Fork. To gain an insight into the mechanistic role of the Mcm4 CTD at the stalled replication fork, we performed a chromatin immunoprecipitation (ChIP) assay using cells synchronously entering S phase in the presence of HU (Fig. 5*A*).

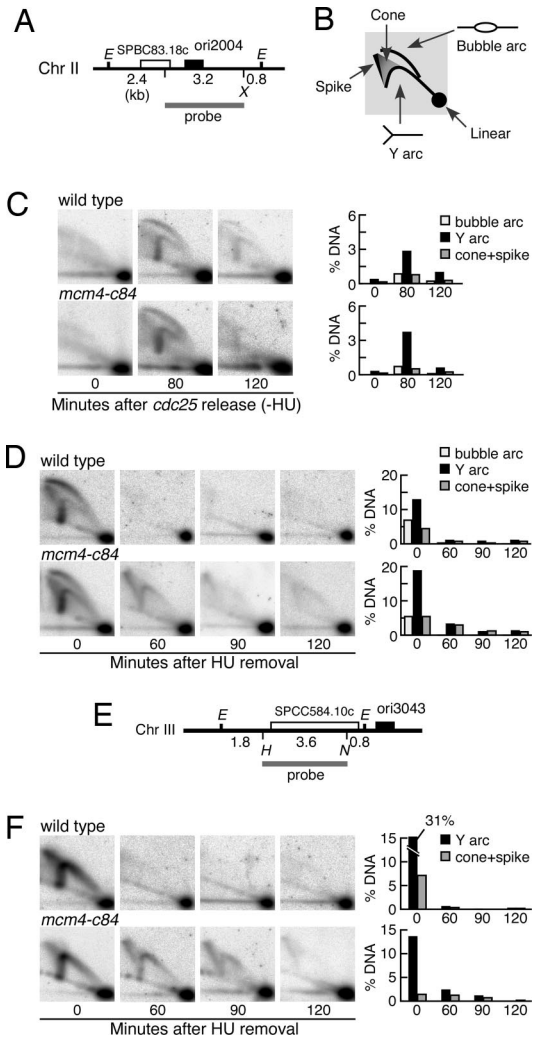

Fig. 4. The Mcm4 CTD is required for the disappearance of the replication intermediates after release from replication block. (*A*) Positions of *ori2004* (filled rectangle), a region used to prepare the probe in Southern blot analysis (gray bar), and the restriction sites (*E*, *EcoT22I*; *X*, *XbaI*) are indicated. (*B*) Schematic diagram of the replication intermediates detected by 2D gel analysis. (*C*) 2D gel analysis of the replication intermediates produced in the absence of HU in wild-type (TNF701) and *mcm4–c84* (TNF1687) cells. Synchronous cultures were obtained by using the *cdc25-22* background strains as described in Fig. 2*B*, except that the synchronous cultures were allowed to enter into S phase in the absence of HU. The cells were collected at the indicated time points after release from *cdc25*-mediated G2 arrest. (*D*) The replication intermediates formed in the restriction fragment containing *ori2004* were detected during recovery from an HU-induced replication block. Yeast cultures were prepared as described in Fig. 2*B*. The cells were collected at the indicated time points after removal of HU from the culture. The proportions of bubble arcs, Y arcs, and cone+spike signals in the total DNA are shown in the graph. (*E*) The positions of *ori3043* (filled rectangle), a region used to prepare the probe in Southern blot analysis (gray bar), and the restriction sites (*E*, *EcoT22I*; *H*, *Hin*dIII; *N*, *Nhe*I) are indicated. (*F*) The replication intermediates formed in the origin-free fragment were detected during recovery from an HU-induced replication block. The graph shows the proportion of Y arcs and cone+spike signals in the total DNA.

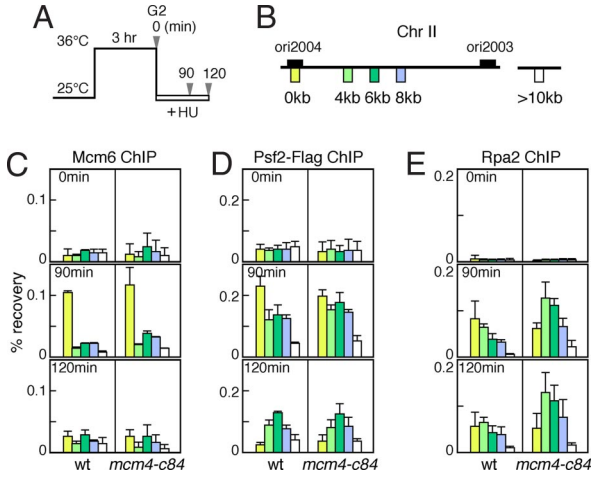

Fig. 5. Association of Mcm6, Psf2-Flag, and Rpa2 around *ori2004* on chromosome II in the presence of HU. (*A*) Schematic diagram to prepare *cdc25-22* cultures that synchronously enter into S phase in the presence of HU. After incubation at 36°C, 10 mM HU was added to the culture, and the temperature was decreased to 25°C. The cells were harvested at the indicated time points. (*B*) The regions of chromosome II that were amplified by qPCR are indicated. The >10-kb region is located at the chromosome site where no origins are present within 10 kb on either side (42). The positions of *ori2004* and *ori2003* are also shown. The wild-type (TNF2164) and *mcm4–c84* (TNF2165) strains containing the *psf2-3flag* gene (32) were used for Mcm6 and Psf2-Flag ChIP; wild-type (TNF701) and *mcm4–c84* (TNF1687) strains were used for Rpa2 ChIP. (*C*) Chromatin binding of Mcm6. (*D*) Chromatin binding of Psf2-Flag. (*E*) Chromatin binding of Rpa2. The percentage of recovered DNA compared with the input is shown. The colors of the bars indicate the position of the chromosomal regions (*B*) amplified by qPCR. The values represent the mean of two independent experiments; the error bars represent the standard deviation. wt, wild-type.

Four different regions around *ori2004* and a region >10 kb away from an origin were examined by quantitative PCR (qPCR) (Fig. 5*B*). By using antibodies against Mcm6, binding to *ori2004* in early S phase was observed similarly in wild-type and *mcm4–c84* cells (Fig. 5*C*, 90 min), suggesting that *mcm4–c84* does not affect pre-RC formation. Binding of Mcm6 to the regions outside of the origin was hardly detected in this study. Thus, we could not examine Mcm6 binding at the fork. The GINS complex is loaded onto the pre-RC and becomes an essential component of the DNA-unwinding machinery (5, 32). To determine whether *mcm4–c84* affects the unwinding machinery, we examined the chromatin binding of Psf2, a subunit of GINS. The tagged Psf2-Flag was immunoprecipitated by using anti-Flag antibody. As observed in the case of Mcm6, Psf2-Flag transiently bound to *ori2004* (Fig. 5*D*, 90 min). Furthermore, the binding of Psf2-Flag to regions outside *ori2004* was also detected and was most prominent at the 6-kb region at a later time point (120 min). These observations are consistent with the idea that Psf2 is a component of the DNA-unwinding machinery. We found that *mcm4–c84* does not affect Psf2-Flag chromatin binding, suggesting that the Mcm4 CTD is not required to maintain the unwinding machinery on the stalled forks. Finally, we examined the chromatin binding of Rpa2, a subunit of the ssDNA-binding protein RPA. After entry into S phase, Rpa2 was detected around *ori2004* (Fig. 5*E*). Although *mcm4–c84* did not change Rpa2 binding at *ori2004*, it increased Rpa2 binding at regions 4 or 6 kb away from *ori2004*, indicating that excessive amounts of ssDNA are produced near *ori2004*. Similar results were obtained around a different origin of replication (Fig. S2). These data suggest that the Mcm4 CTD prevents excessive formation of ssDNA at stalled replication forks.

Discussion

MCM helicase is an essential component of the DNA replication fork. Among subunits Mcm2–7, Mcm4 is the most highly conserved throughout evolution. Here, we found that truncations of the Mcm4 CTD (*mcm4–c84* and *mcm4–c70*) resulted in hypersensitivity to a replication block induced by dNTP depletion but caused no apparent growth defects under unperturbed condi-

tions. Because *mcm4–c84* does not affect Mcm6 and Psf2 loading onto the origins and the formation of replication intermediates, it is unlikely that the sensitivity to dNTP depletion is because of a reduction in replication initiation. An intimate relationship between MCM and the replication checkpoint has been reported (33–36). However, *mcm4–c84* does not affect HU-induced phosphorylation of Cds1 and Mus81, which occurs in a Rad3- and Cds1-dependent manner, respectively. In addition, the kinase activity of Cds1 is increased to the wild-type level. When the Cds1 pathway is impaired, the DNA damage checkpoint kinase Chk1 becomes activated in response to HU; however, Chk1 phosphorylation is suppressed in *mcm4–c84* as well as in wild-type cells. Finally, *mcm4–c84* further increases the HU sensitivity of the checkpoint mutants. These data show that the Mcm4 CTD plays a role other than in activation of the replication checkpoint when replication is blocked by dNTP depletion.

The Mcm4 CTD is required for efficient recovery of stalled replication forks after release from the replication block. The *mcm4–c84* mutation causes a delay in the disappearance of replication intermediates and attenuation of the replication checkpoint kinase Cds1. The residual activity of Cds1 kinase may be because of the stalled forks remaining after HU removal. Although it cannot be formally excluded, it is unlikely that the replication machinery is collapsed in *mcm4–c84* cells because *mcm4–c84* does not affect the association of Psf2 to stalled forks. Full activation of the replication checkpoint and suppression of the DNA damage checkpoint support the notion that the replication machinery is not disrupted in *mcm4–c84* cells. Remarkably, we found that the *mcm4* mutation of MCM helicase brings about an increase rather than a decrease in the binding of Rpa2 to stalled forks, indicating that the Mcm4 CTD suppresses excessive ssDNA formation. Electron microscopic studies have shown that HU treatment increases the length of ssDNA at the fork by ≈100 nt (20). Because *mcm4–c84* causes a ≈2-fold increase in Rpa2 binding near the origin, it appears that ssDNA at the stalled fork is extended to 200 nt. This relatively small difference may explain why *mcm4–c84* does not drastically change the Psf2 binding site in the ChIP assay. Alternatively, it is possible that *mcm4–c84* increases the number of forks that have an extended length of ssDNA, rather than the length of ssDNA at a fork. In either case, down-regulation of DNA unwinding is relieved by *mcm4–c84*. It has been observed that Mrc1, Swi1, and Swi3 prevent uncoupling of DNA synthesis and the replication machinery (37, 38). As in the case of *mrc1*Δ cells (18), the HU sensitivity of *mcm4–c84* cells can be partially suppressed by a mutation in Cdc45, a component of the unwinding machinery, but not by a mutation in Orc1, a subunit of the origin recognition complex (Fig. S3). However, *mcm4–c84* enhances the HU sensitivity of *mrc1*Δ, *swi1*Δ, and *swi3*Δ cells, suggesting that the Mcm4 CTD plays a role related, but not identical, to that of Mrc1, Swi1, or Swi3 (Fig. S4). Recent studies of archaeal Mcm have shown that truncation of its CTD increases ATPase and DNA unwinding activities (39, 40). Given the sequence similarity between archaeal Mcm and eukaryotic Mcm4s, the function of the CTD appears to be conserved across kingdoms. Our findings suggest that after the formation of ssDNA sufficient for checkpoint activation, Mcm4 CTD suspends the DNA unwinding activity of MCM helicase.

Materials and Methods

Yeast Strains and Plasmids. The yeast strains used in this study are listed in Table S1. The media were prepared as described elsewhere (18). The *mcm4–c70*, *mcm4–c84*, and *mcm4–c106* mutants were created by yeast transformation with *Spe*I-digested pTN565, and *Xba*I-digested pTN558 and pTN559, respectively. These plasmids were constructed as follows. Introducing the *Bgl*II-*Eco*RI restriction sites immediately after the *mcm4* stop codon, a 1.3-kb *Eco*RV-*Bam*HI fragment containing the Mcm4 C-terminal region was amplified by PCR and then cloned between the EcoRV and BamHI of pBluescript II KS$^+$, creating pTN528. A 1.5-kb *Bgl*II-*Eco*RI fragment containing kanMX6 from pFA6-kanMX6 (41) was cloned into the *Bgl*II and *Eco*RI sites of pTN528, creating pTN529. The reverse primer (5′-AACAGCTATGACCATG) was paired with the forward mutagenesis primer mcm4-cd70 [5′-CGAGATC*TTA*GACCATATCTTCAGGTACCAAAG (the underlined portion represents the *Bgl*II site, and the italicized portion represents the stop codon that was introduced)], mcm4–cd84 (5′-CGAGATC*TTAAATTA*GGTCAAGAGAAATCTTTCC), or mcm4–cd106 (5′-CGAGATC*TTA*CAAGCGAGCAGCTTCAAGAACATC) in PCRs using pTN529 as a template. The PCR products were digested with *Xho*I and *Bgl*II, and the resulting 1.1-kb *Xho*I-*Bgl*II fragments were introduced into the *Xho*I and *Bgl*II sites of pTN529 to create pTN565, pTN558, and pTN559, respectively. The absence of any additional mutations in the PCR fragment was confirmed by DNA sequencing. A 4.3-kb region of yeast genomic DNA that contains SPCC584.10c was amplified by using a pair of primers (5′-CGCAAGGGCGTCGTTACCCATGG and 5′-CTCAACTACCGGCTAAGGTTGGC), digested with *Hin*dII and *Nhe*I, and the resulting 3.6-kb *Hin*dIII-*Nhe*I fragment was introduced into the *Hin*dIII and *Xba*I sites of pBluescript II KS$^+$, creating pTN807.

Doubling Time of Yeast Cells. Late log-phase cultures of yeast cells in EMM media were diluted with fresh EMM to a final concentration of 3.0×10^6 cells per ml. Thereafter, the cell concentration was determined at 1-h intervals for 7 h.

Preparation of Yeast Extracts. Yeast extracts were prepared as described previously (18), except for the addition of 3 μl of phosphatase inhibitor mixture (Sigma) before cell disruption.

***In Vitro* Cds1 Kinase Assay.** The *in vitro* Cds1 kinase assay was performed as described previously (18).

2D Gel Electrophoresis. Neutral-neutral 2D gel electrophoresis was carried out as described elsewhere (42). For Southern blotting, a 3.2-kb *Not*I-*Xba*I fragment from pXN289 (43) and a 3.6-kb *Hin*dIII-*Not*I fragment from pTN807 were labeled with ^{32}P using the Megaprime DNA labeling system (GE Healthcare) to detect the 6.4- and 6.2-kb *Eco*T22I fragments containing *ori2004* and SPCC584.10c, respectively. The radioactive signals were detected with a BAS 2500 phosphorimager (Fuji) and measured by using Image Gauge software (Fuji).

ChIP. ChIP experiments were performed as described previously (42). Immunoprecipitation was carried out by using anti-Mcm6 (44) or anti-Rpa2 (32) rabbit serum preincubated with magnetic beads conjugated to sheep anti-rabbit IgG (Dynabeads M-280; Invitrogen) or by using anti-Flag mouse monoclonal antibody M2 (Sigma) preincubated with the magnetic beads conjugated to sheep anti-mouse IgG (Dynabeads M-280). To measure the DNA concentration, qPCR was performed by using Power SYBR green PCR master mix and a 7300 PCR system (Applied Biosystems). The primer sequences have been enumerated in Table S2.

ACKNOWLEDGMENTS. We thank P. Russell (The Scripps Research Institute, La Jolla, CA) and P. Nurse (Rockefeller University, New York, NY) for strains; K. Tanaka (Kansei Gakuin Unversity, Hyogyo, Japan) for plasmids; T. S. Wang (Stanford University, Stanford, CA) for antibodies; and T. Takahashi (Osaka University, Osaka, Japan) for critical reading of the manuscript. This work was supported by a Grant-in-Aid for Cancer Research from the Ministry of Education, Culture, Sports, Science and Technology and funding from the Sumitomo Foundation and the Naito Foundation (to T.N.).

1. Kolodner RD, Putnam CD, Myung K (2002) Maintenance of genome stability in *Saccharomyces cerevisiae*. *Science* 297:552–557.
2. Bell SP, Dutta A (2002) DNA replication in eukaryotic cells. *Annu Rev Biochem* 71:333–374.
3. Arias EE, Walter JC (2007) Strength in numbers: Preventing rereplication via multiple mechanisms in eukaryotic cells. *Genes Dev* 21:497–518.
4. Moyer SE, Lewis PW, Botchan MR (2006) Isolation of the Cdc45/Mcm2–7/GINS (CMG) complex, a candidate for the eukaryotic DNA replication fork helicase. *Proc Natl Acad Sci USA* 103:10236–10241.
5. Gambus A, *et al.* (2006) GINS maintains association of Cdc45 with MCM in replisome progression complexes at eukaryotic DNA replication forks. *Nat Cell Biol* 8:358–366.
6. Pacek M, Tutter AV, Kubota Y, Takisawa H, Walter JC (2006) Localization of MCM2–7, Cdc45, and GINS to the site of DNA unwinding during eukaryotic DNA replication. *Mol Cell* 21:581–587.
7. Yoshida K, Inoue I (2003) Conditional expression of MCM7 increases tumor growth without altering DNA replication activity. *FEBS Lett* 553:213–217.
8. Honeycutt KA, *et al.* (2006) Deregulated minichromosomal maintenance protein MCM7 contributes to oncogene driven tumorigenesis. *Oncogene* 25:4027–4032.

9. Shima N, *et al.* (2007) A viable allele of Mcm4 causes chromosome instability and mammary adenocarcinomas in mice. *Nat Genet* 39:93–98.
10. Ivessa AS, *et al.* (2003) The *Saccharomyces cerevisiae* helicase Rrm3p facilitates replication past nonhistone protein-DNA complexes. *Mol Cell* 12:1525–1536.
11. Branzei D, Foiani M (2005) The DNA damage response during DNA replication. *Curr Opin Cell Biol* 17:568–575.
12. Lopes M, *et al.* (2001) The DNA replication checkpoint response stabilizes stalled replication forks. *Nature* 412:557–561.
13. Carr AM (2002) DNA structure dependent checkpoints as regulators of DNA repair. *DNA Repair* 1:983–994.
14. Lindsay HD, *et al.* (1998) S-phase-specific activation of Cds1 kinase defines a subpathway of the checkpoint response in *Schizosaccharomyces pombe. Genes Dev* 12:382–395.
15. Boddy MN, Furnari B, Mondesert O, Russell P (1998) Replication checkpoint enforced by kinases Cds1 and Chk1. *Science* 280:909–912.
16. Shimada K, Pasero P, Gasser SM (2002) ORC and the intra-S-phase checkpoint: A threshold regulates Rad53p activation in S phase. *Genes Dev* 16:3236–3252.
17. Tercero JA, Longhese MP, Diffley JF (2003) A central role for DNA replication forks in checkpoint activation and response. *Mol Cell* 11:1323–1336.
18. Nitani N, Nakamura K, Nakagawa C, Masukata H, Nakagawa T (2006) Regulation of DNA replication machinery by Mrc1 in fission yeast. *Genetics* 174:155–165.
19. Byun TS, Pacek M, Yee MC, Walter JC, Cimprich KA (2005) Functional uncoupling of MCM helicase and DNA polymerase activities activates the ATR-dependent checkpoint. *Genes Dev* 19:1040–1052.
20. Sogo JM, Lopes M, Foiani M (2002) Fork reversal and ssDNA accumulation at stalled replication forks owing to checkpoint defects. *Science* 297:599–602.
21. Zou L, Elledge SJ (2003) Sensing DNA damage through ATRIP recognition of RPA-ssDNA complexes. *Science* 300:1542–1548.
22. Kearsey SE, Labib K (1998) MCM proteins: Evolution, properties, and role in DNA replication. *Biochim Biophys Acta* 1398:113–136.
23. Neuwald AF, Aravind L, Spouge JL, Koonin EV (1999) AAA$^+$: A class of chaperone-like ATPases associated with the assembly, operation, and disassembly of protein complexes. *Genome Res* 9:27–43.
24. Fletcher RJ, *et al.* (2003) The structure and function of MCM from archaeal *M. thermoautotrophicum. Nat Struct Biol* 10:160–167.
25. Fernandez Sarabia MJ, McInerny C, Harris P, Gordon C, Fantes P (1993) The cell cycle genes *cdc22*$^+$ and *suc22*$^+$ of the fission yeast *Schizosaccharomyces pombe* encode the large and small subunits of ribonucleotide reductase. *Mol Gen Genet* 238:241–251.
26. Lindner K, Gregan J, Montgomery S, Kearsey SE (2002) Essential role of MCM proteins in premeiotic DNA replication. *Mol Biol Cell* 13:435–444.
27. Tanaka K, Boddy MN, Chen XB, McGowan CH, Russell P (2001) Threonine-11, phosphorylated by Rad3 and ATM *in vitro*, is required for activation of fission yeast checkpoint kinase Cds1. *Mol Cell Biol* 21:3398–3404.
28. Kai M, Boddy MN, Russell P, Wang TS (2005) Replication checkpoint kinase Cds1 regulates Mus81 to preserve genome integrity during replication stress. *Genes Dev* 19:919–932.
29. Xu YJ, Davenport M, Kelly TJ (2006) Two-stage mechanism for activation of the DNA replication checkpoint kinase Cds1 in fission yeast. *Genes Dev* 20:990–1003.
30. Brewer BJ, Fangman WL (1987) The localization of replication origins on ARS plasmids in *S. cerevisiae. Cell* 51:463–471.
31. Lopes M, Cotta-Ramusino C, Liberi G, Foiani M (2003) Branch migrating sister chromatid junctions form at replication origins through Rad51/Rad52-independent mechanisms. *Mol Cell* 12:1499–1510.
32. Yabuuchi H, *et al.* (2006) Ordered assembly of Sld3, GINS and Cdc45 is distinctly regulated by DDK and CDK for activation of replication origins. *EMBO J* 25:4663–4674.
33. Ishimi Y, Komamura-Kohno Y, Kwon HJ, Yamada K, Nakanishi M (2003) Identification of MCM4 as a target of the DNA replication block checkpoint system. *J Biol Chem* 278:24644–24650.
34. Yoo HY, Shevchenko A, Shevchenko A, Dunphy WG (2004) Mcm2 is a direct substrate of ATM and ATR during DNA damage and DNA replication checkpoint responses. *J Biol Chem* 279:53353–53364.
35. Cortez D, Glick G, Elledge SJ (2004) Minichromosome maintenance proteins are direct targets of the ATM and ATR checkpoint kinases. *Proc Natl Acad Sci USA* 101:10078–10083.
36. Tsao CC, Geisen C, Abraham RT (2004) Interaction between human MCM7 and Rad17 proteins is required for replication checkpoint signaling. *EMBO J* 23:4660–4669.
37. Katou Y, *et al.* (2003) S-phase checkpoint proteins Tof1 and Mrc1 form a stable replication-pausing complex. *Nature* 424:1078–1083.
38. Noguchi E, Noguchi C, McDonald WH, Yates JR III, Russell P (2004) Swi1 and Swi3 are components of a replication fork protection complex in fission yeast. *Mol Cell Biol* 24:8342–8355.
39. Jenkinson ER, Chong JP (2006) Minichromosome maintenance helicase activity is controlled by N- and C-terminal motifs and requires the ATPase domain helix-2 insert. *Proc Natl Acad Sci USA* 103:7613–7618.
40. Barry ER, McGeoch AT, Kelman Z, Bell SD (2007) Archaeal MCM has separable processivity, substrate choice and helicase domains. *Nucleic Acids Res* 35:988–998.
41. Bahler J, *et al.* (1998) Heterologous modules for efficient and versatile PCR-based gene targeting in *Schizosaccharomyces pombe. Yeast* 14:943–951.
42. Hayashi M, *et al.* (2007) Genome-wide localization of pre-RC sites and identification of replication origins in fission yeast. *EMBO J* 26:1327–1339.
43. Okuno Y, Okazaki T, Masukata H (1997) Identification of a predominant replication origin in fission yeast. *Nucleic Acids Res* 25:530–537.
44. Ogawa Y, Takahashi T, Masukata H (1999) Association of fission yeast Orp1 and Mcm6 proteins with chromosomal replication origins. *Mol Cell Biol* 19:7228–7236.